JOURNAL OF AIRCRAFT
Vol. 46, No. 6, November–December 2009

Engineering Notes

Aeroelastic Study of Bistable Composite Airfoils

S. Daynes,* P. M. Weaver,† and K. D. Potter‡
University of Bristol,
Bristol, England BS8 1TR, United Kingdom

DOI: 10.2514/1.44287

Nomenclature

A	=	aerodynamic operator
C_p	=	pressure coefficient
c	=	airfoil chord length
d	=	flap length
F	=	force per unit blade section width
k	=	modal stiffness
Q	=	modal force per unit blade section width
q	=	dynamic pressure
W	=	work per unit blade section width
w	=	vertical displacement
x	=	chordwise position
Θ	=	flap deflection angle
φ	=	airfoil deformation mode

Subscripts

a	=	actuator
b	=	bistable component
f	=	aerodynamic
l	=	lower surface
u	=	upper surface
0	=	denotes zero flap deflection
1, 2	=	bistable geometries

Superscripts

def	=	deflected angle
snap	=	snap-through angle

Introduction

THE most common technique to change the aerodynamic forces acting on an airfoil is to perform a camber change. A conventional way of achieving this movement is with a pin-jointed control surface (i.e., a flap/rudder/aileron) at the trailing edge with a corresponding actuator system. Such solutions require mechanical joints, bearings, movable parts, etc. There can be a significant mass penalty with such components even if the actual structure is optimized for mass. This work presents a design for an airfoil section which has two stable camber geometries. The inherent bistability derives from the use of a bistable laminate known as a prestressed buckled laminate [1,2]. The design of shape adaptive structures requires an understanding of several different disciplines and their various interactions [3]. Lightweight design is an extremely important consideration in the aerospace industry with the aim of creating structures with a high strength-to-weight ratio. However, for adaptive structures, deformability is also a key consideration, which can often be in conflict with the requirement for a lightweight design. Conventional mechanisms, such as flaps, are highly shape adaptable and can carry high loads but cannot be called lightweight. Compliant mechanisms offer the advantage of being both shape adaptable and lightweight. At present, however, the load-carrying capability of compliant mechanisms tends to be relatively poor.

It is instructive to take a historical perspective on the evolution of adaptive structures in the aerospace industry. The original vision of flight was biomimetically inspired from the natural world. This philosophy was quickly abandoned by engineers in the early years of flight in favor of a more conventional mechanical approach to aircraft control. Biomimetic flight control was perhaps not the wrong solution, but just ahead of its time. The earliest solutions tended to make use of flexible elements (i.e., skins or ribs), which can alter large portions of the airfoil geometry [4]. Later design solutions tended to use internal structures with the aim of only creating local deformations in the leading- and/or trailing-edge regions in addition to the use of flexible skins [5–7]. Bistable and multistable structures are good candidates to be used as shape-adaptive structures because of their ability to remain in equilibrium after a shape change occurs [8–11].

The Intelligent Responsive Composite Structures (IRCS) program at the University of Bristol aims to identify methods by which localized segments of an airfoil section may be shape adapted for performance and other advantages. The total IRCS system comprises bi- or multistable composite material constructions that change shape when forced by actuators. The design case here is based on a typical helicopter main rotor blade. The blade section considered is a modestly cambered airfoil section with a chord length c of 680 mm and a maximum thickness-to-chord ratio of 16%. For the purpose of this project, this airfoil geometry is approximated by a NACA 24016 airfoil section with a 15% c flap. The purpose of the IRCS device is to improve the performance of the rotor blade in both the hover and forward flight regimes by having more than one stable shape. The flap is required to be in a stable state at both 0 and $+10$ deg trailing-edge deflection. A positive deflection is defined as vertically downward for the trailing edge (see Fig. 1). The flap then remains in a constant state until actuated, that is, after transit from hover to forward flight, etc. At this point, the bistable structure is actuated to change shape. Changes of camber state are thus relatively infrequent and so a coarse control of the structure (fully off to fully on) can be tolerated.

In this work, the bistable airfoil is considered as a coupled structure-mechanism system. The actuator system and the aerodynamic loads are also coupled to the structure. Such a complex analysis is essential to both understanding the aeroelastic characteristics of the system as well as calculating the mechanical work required from the actuator. The analysis performed in this work is done in two steps:

1) An aeroelastic analysis is presented which couples the adaptive structure with variable aerodynamic loads. An analytical model is formulated to model the interaction between the structural and aerodynamic stiffnesses.

2) The aerodynamic loads are estimated using a numerical example. Inviscid calculations of the aerodynamic pressure distributions

Received 11 March 2009; revision received 6 August 2009; accepted for publication 25 August 2009.

*Ph.D. Student, Department of Aerospace Engineering, Queen's Building. Member AIAA.

†Professor, Department of Aerospace Engineering, Queen's Building. Member AIAA.

‡Reader, Department of Aerospace Engineering, Queen's Building.

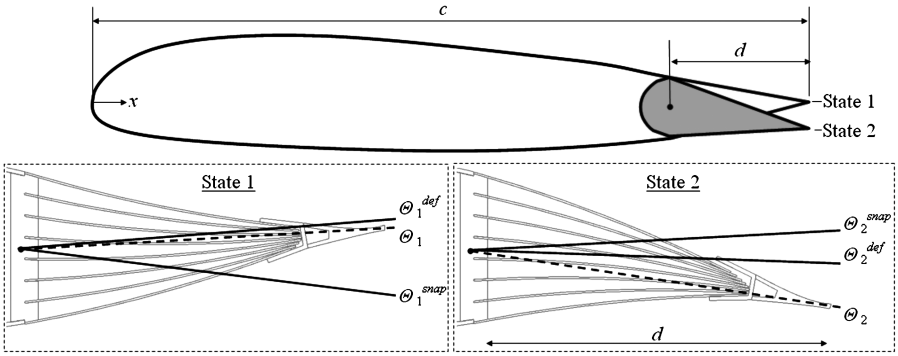

Fig. 1 Camber change region on rotor blade.

around the airfoil are then carried out. This is done using the computational fluid dynamics (CFD) software XFOIL [12]. The load carrying capability of the structure is then assessed.

The novelty of this current work lies in the fact that the airfoil flap can remain in one of two stable geometries and both states are able to withstand the aerodynamic loading without any additional holding forces or locking mechanisms. An actuator is only required during transition between these two stable geometries.

Structural Design

The airfoil section with a bistable flap manufactured is shown in Fig. 2. The bistable flap consists of a stack of six bistable prestressed buckled laminates. The details of the modeling and manufacturing of these bistable laminates are described in [1]. The plates have dimensions of 100×100 mm and are made from Hexcel 913 glass fiber reinforced plastic (GFRP) prepreg [13]. The selected lay-up is $[0/90/90/0]_T$ for each plate with prestressing being applied in the 0 deg direction. For these plates, 1.1% prestrain in total was applied during manufacture (see Fig. 3). The 90 deg fibers are spanwise to the rotor. It was found that prestressing half of the 0 deg plies with this lay-up and magnitude of prestress produced the desired 10 deg change in flap angle while requiring large snap-through moments to change between stable states. The upper and lower external skins of the flap are manufactured from the same GFRP prepreg but are not bistable and have the lay-up $[90/0/90]_T$. In the undeformed configuration, the external skin follows a near identical profile to the standard rotor blade section. In the deformed configuration, this external skin creates a continuous camber change, unlike a conventional flap solution which cambers at a discrete point. This design feature has the potential to improve aerodynamic effects such as the point of trailing-edge separation and localized pressure spikes.

The bistable plates are attached at one of their ends to a spar situated at 85% chord on the rotor blade. The attachments are restricted to dimensions of 5 mm width to ensure the bistable behavior of the plates is not significantly affected in one or both of their stable states. The arrangement of the bistable plates made by the spar resembles a fan due to the angles at which the plates are clamped. The angles selected intersect slightly before the trailing edge. This feature has the effect of forcing the bistable plates together, making a stiffer trailing edge. There is a requirement for a discontinuity in the skin at the trailing edge because there is a corresponding relative change in length of the external skin between the upper and lower surfaces during transition between stable modes. This complication is unavoidable due to the restrictive geometry a cambering airfoil presents. Because this design feature is unavoidable, a skin discontinuity at the trailing edge is aerodynamically (and structurally) the most desirable solution to the problem. Foam tape has been placed between each of the plates at the trailing edge. The foam material makes the airfoil weathertight and minimizes friction between the plates. The low shear stiffness of foam does not restrict the plates from sliding over each other significantly. In practice, a sharp, solid, trailing edge would be added, as shown in Fig. 1, but this was omitted from the flap demonstrator model because it does not contribute to the snap-through stiffness of the flap.

To quantify the structural stiffnesses and snap-through characteristics of the bistable flap, the manufactured airfoil was subject to a set of load-displacement tests. The manufactured airfoil was mounted over the static crosshead of an INSTRON type 3343 1 kN test machine. The bistable plate spar was mounted so as to be parallel to the direction of motion of the moving crosshead of the test machine. Compressive load was applied to the flap using a small metal pointer so as to obtain load-displacement data (see Fig. 4a). For practical purposes, the test machine's frame is assumed to be completely rigid. The rotor blade section consists of a leading-edge composite D-spar and a honeycomb-composite sandwich structure between the two spars. It is assumed that this structure in front of the flap region is also rigid relative to the compliant flap, an assumption that is validated by wind-tunnel testing [14]. From this force-displacement data and knowledge that the flap is 100 mm long, force-rotation data were obtained. Four compressive force-displacement tests were carried out: two tests in opposing directions for both flap states. From these four tests, a hysteresis loop describing the force-rotation characteristics of the bistable airfoil was constructed, as shown in Fig. 4b. From Fig. 4b, it is clear that two stable flap angles Θ exist when the applied force per unit blade section width F_b is zero. These are called flap state 1 ($\Theta_1 = 0$ deg) and flap state 2 ($\Theta_2 = 10$ deg). For small displacements, each of these flap states can be assigned a modal stiffness k_b and a critical angle of deflection at which snap-through occurs, Θ_1^{snap} and Θ_2^{snap} for the two states, respectively. For small flap

Structural Design

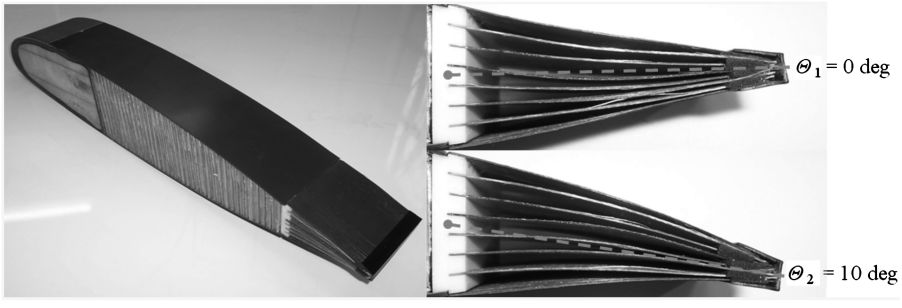

Fig. 2 Rotor blade section with bistable flap.

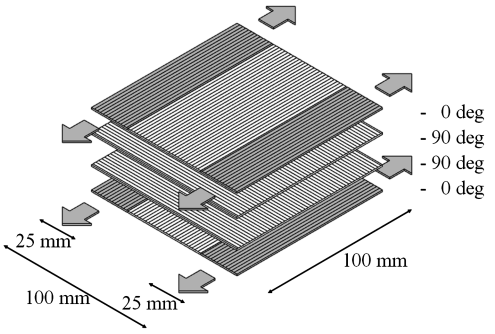

Fig. 3 Lay-up of $[0/90/90/0]_T$ prestressed buckled laminate.

deflections, the modal stiffness of this bistable flap in both states is calculated to be 28.0 N/m/ deg. The two snap-through angles Θ_1^{snap} and Θ_2^{snap} are estimated as 10.2 and −2.3 deg, respectively.

Aeroelastic Analysis

The following theory is adapted from the approach used by Campanile and Anders in the modeling of shape adaptable airfoils [15]. A conventional airfoil section with a pinned flap is shown in Fig. 1. The airfoil chord is denoted by c and the flap length by d. The vertical displacement w is expressed as

$$w(x) = \Theta d\varphi(x) \tag{1}$$

with the origin at the leading edge and $\varphi(x)$ given by

$$\varphi(x) = \begin{cases} 0 & 0 \le x < c-d \\ \frac{x-c+d}{d} & c-d \le x < c \end{cases} \tag{2}$$

and Θ is the flap deflection angle. For small flap rotations, it is assumed that $\sin\Theta = \Theta$. Because it is assumed that the bistable airfoil is a 1-degree-of-freedom system, then the vertical displacement for this case can also be described using a flap deflection angle Θ, a reference length c, and the deformation mode φ. Note that the deformation mode is normalized at the trailing edge such that $\varphi(c) = 1$. Therefore, the modal displacement Θ is equal to the ratio between the trailing-edge displacement and the reference length c. This formulation allows the morphing geometry of the airfoil to be described analytically in terms of a pin-jointed flap.

Work Done by Aerodynamic Loads

The virtual work per unit length δW_f, which is produced by the modal aerodynamic force Q_f on the virtual displacement $\delta\Theta$, is defined as

$$\delta W_f = dQ_f \delta\Theta \tag{3}$$

with

$$Q_f = q\int_0^c (-C_{pu}(x) + C_{pl}(x))\varphi(x)\mathrm{d}x \tag{4}$$

where $C_{pu}(x)$ and $C_{pl}(x)$ are the pressure coefficients for the upper and lower surfaces of the airfoil, respectively, and q is the dynamic pressure. Aeroelastic effects occur when the aerodynamic forces depend on the airfoil deformation. This coupling phenomenon may be represented by a linear aerodynamic operator $A[.]$, as proposed by Campanile and Anders [15], which may be determined empirically using CFD or airfoil section theory. For current purposes, the inviscid aerodynamic characteristics of the airfoil section are known for two different camber configurations from inviscid CFD modeling. Therefore, a linear interpolation can be done between the two data sets for $\Theta = 0$ deg and $\Theta = 10$ deg. The validity of this assumption was tested by comparing the interpolated values of C_p at $\Theta = 5$ deg with those values obtained directly from a CFD model with $\Theta = 5$ deg. A negligible difference was found. The change in pressure coefficients for the upper and lower side of the airfoil can therefore be expressed as a function of the vertical displacement along the chord using the following two linear aerodynamic operators:

$$\Delta C_{pu}(x) = A_u[w(x)] \tag{5}$$

$$\Delta C_{pl}(x) = A_l[w(x)] \tag{6}$$

where ΔC_{pu} and ΔC_{pl} are the change in pressure coefficients for the upper and lower surfaces, respectively. In light of Eqs. (5) and (6), the pressure coefficients for the upper and lower sides of the airfoil are

$$C_{pu}(x) = A_u[\varphi(x)]\Theta + C_{pu0}(x) \tag{7}$$

$$C_{pl}(x) = A_l[\varphi(x)]\Theta + C_{pl0}(x) \tag{8}$$

where $C_{pu0}(x)$ and $C_{pl0}(x)$ are the pressure coefficients for the undeformed airfoil. Similar to Eqs. (7) and (8), the modal aerodynamic force can be written as

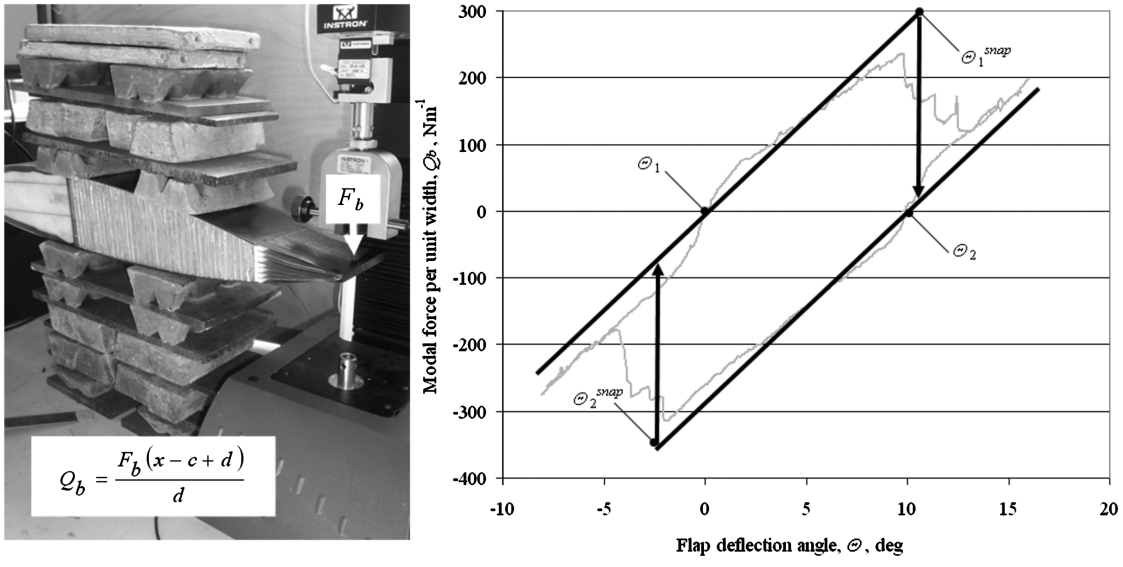

a) b)

Fig. 4 Determination of flap stiffness showing a) experimental setup, and b) results.

$$Q_f = k_f\Theta + Q_{f0} \tag{9}$$

where k_f is the modal aerodynamic stiffness. This modal aerodynamic stiffness is now considered as a function of the airfoil deformation

$$k_f = q\left[\int_0^c (-A_u[\varphi(x)] + A_l[\varphi(x)])\varphi(x)\mathrm{d}x\right] \tag{10}$$

and the modal aerodynamic force for the undeformed airfoil is

$$Q_{f0} = q\left[\int_0^c (-C_{pu0}(x) + C_{pl0}(x))\varphi(x)\mathrm{d}x\right] \tag{11}$$

The terms k_f and Q_{f0} relate to a specific angle of attack. Considering Eqs. (9–11), the aerodynamic work done on the structure W_f in state n between an unloaded flap at an initial flap angle Θ_n and a deflected flap angle Θ_n^{def} can therefore be expressed as

$$W_f = d\int_{\Theta_n}^{\Theta_n^{\mathrm{def}}} Q_f\mathrm{d}\Theta = \frac{d}{2}[Q_{f0}\Theta + k_f(\Theta_n + \Theta)\Theta]_{\Theta_n}^{\Theta_n^{\mathrm{def}}} \tag{12}$$

Work Done on Deformation of Flap

The virtual work per unit length δW_b, which is produced by the modal bistable plate force Q_b on the virtual displacement $\delta\Theta$, is defined as

$$\delta W_b = dQ_b\delta\Theta \tag{13}$$

with

$$Q_b = F_b\varphi \tag{14}$$

where F_b is the force per unit width reacted by the bistable plates (see Fig. 4a). The modal force Q_b is a function of flap angle Θ. Assuming small deflections, Q_b can be described by

$$Q_b = k_b\Theta \tag{15}$$

where k_b is the modal stiffness of the bistable flap. Values of k_b can be found from the gradients of force-flap deflection relationships shown in Fig. 4b. Identical values of k_b are assigned to both stable configurations for this flap, noting that, in general, they could be different if required. The work done to deform the structure W_b, in terms of the flap deflection angle of the structure in state n between an initial flap angle Θ_n and a deflected flap angle Θ_n^{def}, can therefore be expressed as

$$W_b = d\int_{\Theta_n}^{\Theta_n^{\mathrm{def}}} Q_b\mathrm{d}\Theta = \frac{dk_b}{2}[\Theta^2]_{\Theta_n}^{\Theta_n^{\mathrm{def}}} \tag{16}$$

Calculation of Initial Deflection Angle

For the flap to be in equilibrium without any actuator input, the sum of the work done on the structure by the aerodynamic loads W_f and the work done on the aerodynamic loads by the structure W_b is zero:

$$W_f + W_b = 0 \tag{17}$$

The initial deflection of the flap under aerodynamic loading without actuation Θ_n^{def} in state n is therefore found by substituting Eqs. (12) and (16) into Eq. (17) and rearranging in terms of Θ_n^{def},

$$\Theta_n^{\mathrm{def}} = \Theta_n - \frac{Q_{f0} + k_f\Theta_n}{k_b + k_f} \tag{18}$$

Equation (18) can also predict if snap-through of the flap is going to occur under aerodynamic loading alone. Snap-through of the flap occurs when Θ_n^{def} passes the snap-through angle Θ_n^{snap} for a particular flap state n.

Calculation of Actuator Work

For a conventional airfoil with a pin-jointed flap, no stiffness is associated with change in flap deflection. Therefore, for any configuration, the work done by the actuator W_a must be equal to the aerodynamic work done W_f. The case for the bistable flap is more complicated due to the additional term W_b. The energy input required by the actuator W_a to achieve snap-through can therefore be expressed as

$$W_a = W_f + W_b \tag{19}$$

Before actuation, the flap is in a state of equilibrium at an angle Θ_n^{def}. Therefore, the required work done by the actuator W_a to move the flap from its initial deflected angle Θ_n^{def} to the snap-through angle Θ_n^{snap} can be found using

$$W_a = d\int_{\Theta_n^{\mathrm{def}}}^{\Theta_n^{\mathrm{snap}}} (Q_f + Q_b)\mathrm{d}\Theta = \frac{d}{2}\left(k_f[\Theta^2]_{\Theta_n^{\mathrm{def}}}^{\Theta_n^{\mathrm{snap}}} + k_b|[\Theta^2]_{\Theta_n^{\mathrm{def}}}^{\Theta_n^{\mathrm{snap}}}|\right) \tag{20}$$

The modulus function in Eq. (20) shows that work needs to be done on the structure to rotate the flap in either direction from an equilibrium point, whereas the work done on the aerodynamic loads is dependant on direction. Several bistable plate actuation solutions currently exist. The selection of an actuator will depend on the requirements of the intended application. Actuation could be provided, for example, by using piezoelectric patches [16], shape memory alloy wires [17], or by using an electromechanical actuator [14].

Numerical Example

The design case considered in this numerical example is the blade section at an angle of attack of 15 deg and with a dynamic pressure q of 15 kPa. Approximate chordwise pressure distributions for a NACA 24016 with a 15% chord plain flap are calculated using an inviscid XFOIL model and are shown in Fig. 5. These pressure distributions are both for an angle of attack of 15 deg but with flap deflection angles of $\Theta_1 = 0$ deg and $\Theta_2 = 10$ deg.

From the XFOIL inviscid aerodynamic model and Eqs. (10) and (11), the values of k_f and Q_{f0} are calculated to be 17.0 N/m/ deg and 90.0 N/m, respectively. Numerical results are given in Table 1 where the deflected angles Θ^{def} are found from Eq. (18), the snap-through angles Θ^{snap} are found from Fig. 4b, and the actuator work requirements to achieve snap-through W_a are found from Eq. (20). The analysis predicts that the structure is sufficiently stiff to withstand aerodynamic loading in both stable states without self-actuating. Intuitively, the more highly loaded second stable state shows a greater discrepancy between Θ_n and Θ_n^{def}. This deformation under aerodynamic loading, along with preventing the flap self-actuating, are the key requirements when determining the required modal stiffness of the flap k_b. The analysis also shows that the maximum actuator work needed, under this particular loading regime, is 4.01 J/m to snap the flap from state 1 to state 2. This result is intuitive

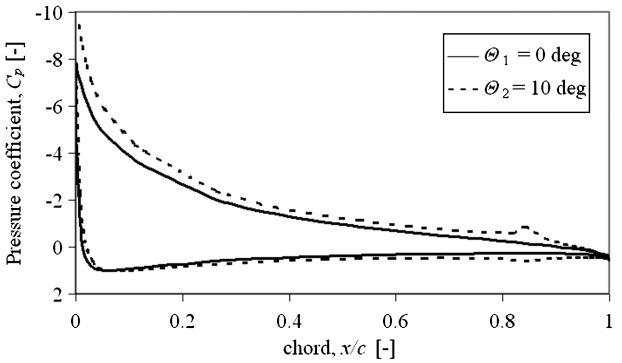

Fig. 5 Pressure distribution over a NACA 24016 with 15 deg angle of attack and $\Theta = 0$ deg and 10 deg.

Table 1 Numerical example results

State	Θ^{def}, deg	Θ^{snap}, deg	W_a, J/m
$\Theta_1 = 0$ deg	−2.00	10.2	4.01
$\Theta_2 = 10$ deg	4.23	−2.3	0.12

because, in this situation, the actuator is required to work not only on deforming the flap, but also against aerodynamic loads. If this design was implemented in practice there will be additional loads caused by the dynamics of the rotor blade system. However, estimation of such loads is beyond the scope of this current work.

Conclusions

A bistable airfoil design has been presented which can change shape between two different camber geometries. An analytical aeroelastic model is presented that couples the structural stiffness of the flap with variable aerodynamic loads depending on camber variation. The formulation of the model allows the required bistable stiffnesses to be easily estimated for the given aerodynamic loads. The trailing edge of the airfoil is able to deflect 10 deg down upon command. The airfoil can remain in either one of its stable states and withstand the perceived maximum aerodynamic loads exerted upon it without the aid of further actuation. In addition to this feature, the design solution presented is lightweight and achieves a smooth camber variation unlike many conventional pin-jointed control surfaces, and so provides favorable aerodynamic flow. Such a bistable device could be used to improve the performance of a rotor blade during the transition between hover and forward flight.

Acknowledgments

The Intelligent Responsive Composite Structures project was partially funded by the U.K. Department for Business, Enterprise, and Regulatory Reform. Intelligent Responsive Composite Structures industrial sponsors include AgustaWestland, GE Aviation, and Garrad-Hassan and Partners, Ltd. The authors thank Dorian Jones at the University of Bristol for his assistance.

References

[1] Daynes, S., Potter, K. D., and "Bistable Prestressed Buckled Laminates," *Composites Science and Technology*, Vol. 68, Nos. 15–16, Dec. 2008, pp. 3431–3437. doi:10.1016/j.compscitech.2008.09.036

[2] Daynes, S., Weaver, P. M., Potter, K. D., and Hardick, M., U.K. Patent Application for "Device Which is Subject to Fluid Flow," Docket No. 0902914.1, filed 20 Feb. 2009.

[3] Campanile, L. F., *Adaptive Structures: Engineering Applications*, Wiley, Chichester, England, U.K., 2007, Chap 4.

[4] Parker, H. F., "The Parker Variable Camber Wing," NACA Rept. No. 77, 1920.

[5] Bilgen, O., Kochersberger, K. B., and Inman, D. J., "A Novel Aerodynamic Vectoring Control Airfoil via Macro-Fiber-Composite Actuators," *49th AIAA/ASME/ASCE/AHS/ASC Structures, Structural Dynamics, and Materials Conference*, Schaumburg, IL, AIAA Paper 2008-1700, 2008.

[6] Baker, D., and Friswell, M. I., "Determinate Structures for Wing Camber Control," *Smart Materials and Structures*, Vol. 18, No. 3, 2009, p. 035014. doi:10.1088/0964-1726/18/3/035014

[7] Kudva, J. N., "Overview of the DARPA Smart Wing Project," *Journal of Intelligent Material Systems and Structures*, Vol. 15, No. 4, April 2004, pp. 261–267. doi:10.1177/1045389X04042796

[8] Bowen, C. R., Butler, R., Jervis, R., Kim, H. A., and Salo, A. I. T., "Morphing and Shape Control using Unsymmetrical Composites," *Journal of Intelligent Material Systems and Structures*, Vol. 18, No. 1, Jan. 2006, pp. 89–98. doi:10.1177/1045389X07064459

[9] Diaconu, C. G., Weaver, P. M., and Mattioni, F., "Concepts for Morphing Airfoil Sections Using Bi-Stable Laminated Composite Structures," *Thin-Walled Structures*, Vol. 46, No. 6, June 2008, pp. 689–701. doi:10.1016/j.tws.2007.11.002

[10] Mattioni, F., Weaver, P. M., and Friswell, M. I., "Modelling and Applications of Thermally Induced Multistable Composites with Piecewise Variation of Lay-Up in the Planform," *48th AIAA/ASME/ASCE/AHS/ASC Structures, Structural Dynamics, and Materials Conference*, Honolulu, HI, AIAA Paper 2007-2262, 2007.

[11] Schultz, M. R., "A Concept for Airfoil-Like Active Bistable Twisting Structures," *Journal of Intelligent Material Systems and Structures*, Vol. 19, No. 2, 2007, pp. 157–169. doi:10.1177/1045389X06073988

[12] Drela, M., and Youngren, H., XFOIL Software Pkg., Ver. 6.9, Dept. of Aeronautics and Astronautics, Massachusetts Inst. of Technology, Cambridge, MA, and AeroCraft, Inc., Portland, ME, 2001.

[13] "HexPly® 913, 125°C Curing Epoxy Matrix, Product Data," Hexcel Corp. Rept. FTA054c, Stamford, CT, March 2007.

[14] Daynes, S., Nall, S. J., Weaver, P. M., Potter, K. D., Margaris, P., and Mellor, P. H., "On a Bistable Flap for an Airfoil," *50th AIAA/ASME/ASCE/AHS/ASC Structures, Structural Dynamics, and Materials Conference*, Palm Springs, CA, AIAA Paper 2009-2103, 2009.

[15] Campanile, L. F., and Anders, S., "Aerodynamic and Aeroelastic Amplification in Adaptive Belt-Rib Airfoils," *Journal of Aerospace Science and Technology*, Vol. 9, No. 1, Jan. 2005, pp. 55–63. doi:10.1016/j.ast.2004.07.007

[16] Schultz, M. R., Hyer, M. W., Williams, R. B., Keats Wilkie, W., and Inman, D. J., "Snap-Through of Unsymmetric Laminates Using Piezocomposite Actuators," *Composites Science and Technology*, Vol. 66, No. 14, Nov. 2006, pp. 2442–2448. doi:10.1016/j.compscitech.2006.01.027

[17] Dano, M.-L., and Hyer, M. W., "SMA-Induced Snap-Through of Unsymmetric Fiber-Reinforced Composite Laminates," *International Journal of Solids and Structures*, Vol. 40, No. 22, Nov. 2003, pp. 5949–5972. doi:10.1016/S0020-7683(03)00374-3